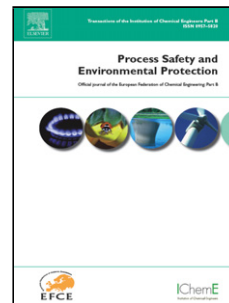


Accepted Manuscript

Title: Long-term dust generation from silicon carbide powders

Authors: Somik Chakravarty, Marc Fischer, Pablo García-Triñanes, Morgane Dalle, Laurent Meunier, Olivier Aguerre-Chariol, Olivier Le Bihan, Martin Morgeneyer



PII: S0957-5820(18)30024-7
DOI: <https://doi.org/10.1016/j.psep.2018.01.021>
Reference: PSEP 1286

To appear in: *Process Safety and Environment Protection*

Received date: 9-11-2017
Revised date: 24-1-2018
Accepted date: 30-1-2018

Please cite this article as: Chakravarty, Somik, Fischer, Marc, García-Triñanes, Pablo, Dalle, Morgane, Meunier, Laurent, Aguerre-Chariol, Olivier, Bihan, Olivier Le, Morgeneyer, Martin, Long-term dust generation from silicon carbide powders. *Process Safety and Environment Protection* <https://doi.org/10.1016/j.psep.2018.01.021>

This is a PDF file of an unedited manuscript that has been accepted for publication. As a service to our customers we are providing this early version of the manuscript. The manuscript will undergo copyediting, typesetting, and review of the resulting proof before it is published in its final form. Please note that during the production process errors may be discovered which could affect the content, and all legal disclaimers that apply to the journal pertain.

Long-term dust generation from silicon carbide powders

Somik Chakravarty^{#,*}, Marc Fischer^{†,*}, Pablo García-Triñanes[^], Morgane Dalle[†], Laurent Meunier[†], Olivier Aguerre-Chariol[†], Olivier Le Bihan[†] and Martin Morgeneyer^{*}

^{*} Université de Technologie de Compiègne (UTC) - Sorbonne Universités, Laboratoire Transformations intégrées de la matière renouvelable (TIMR), Rue Roger Couitolenc, CS 60319, 60203 Compiègne Cedex, France
e-mail: somik.chakravarty@utc.fr, web page: <http://www.utc.fr/>

[†] Institut National de l'Environnement Industriel et des Risques (INERIS), NOVA/CARA/DRC/INERIS, Parc Technologique Alata, BP2, F-60550 Verneuil-En-Halatte, France

[^] Wolfson Centre of Bulk Solid Handling Technology, Faculty of Engineering and Science, University of Greenwich, Chatham Maritime, Chatham, Kent ME4 4TB, UK

Abstract

Most dustiness studies do not measure dust release over long durations, nor do they characterize the effect of dust release on bulk powders. In this study, we tested the dustiness of two different samples of silicon carbide (SiC) powders (referred to as F220 and F320) over six hours using a vortex shaker. Additionally, we characterized the bulk sample for change in shape and size distribution due to the testing. Both powders release respirable fractions of dust particles but differ in their dust generation behavior. The numbers of released respirable particles for powder F220 are more than two times higher than those of powder F320.

The dust generation mechanism might include the release of aerosols due to the attrition of particles owing to inter-particle and particle-wall impaction. This study emphasizes the need for long duration dustiness tests for hard materials like SiC and characterization for change in bulk material properties due to dust generation and release. Furthermore, the results can aid in selecting the bulk material for long-term applications based on dustiness.

Keywords: Dustiness, Silicon carbide particles, Vortex shaker, Attrition, Dust generation mechanism.

1. Introduction

Hard particles, such as silicon carbide (SiC) having diameters in the range of 30-100 μm are widely used in high endurance applications such as the production of abrasives and wear-resistant machineries (Harris, 1995). Considering their excellent physical and mechanical properties (high strength, durability and heat capacity), SiC powders have recently been adopted as a heat transfer and storage fluid (HTF) for concentrated solar thermal plants (CSP) (Benoit et al., 2015; García-Triñanes et al., 2016). The HTF particles conveyed pneumatically or mechanically are used to transfer heat energy from different sections of the solar thermal plant. The conveying of HTF material generates dust as it undergoes mechanical stresses due to screw feeder or rotary valves, kinetic stresses due to high-velocity jets, conveyors, collision with tubes, and shear stresses while being conveyed in a closed circulating loop. Further, such stresses engender attrition in particulate systems which can potentially influence the physical, mechanical and thermal properties of the HTF material and therefore, the operation of the CSP plant. Thus, the handling of such material requires the knowledge of the powder ability to generate dust and monitor its consequent change in physical and mechanical properties which may be different from their original state.

According to ISO 4225 (International Organization for Standardization, 1994), dust is made of small airborne solid particles, usually of sizes inferior to 75 μm in diameter which settle under their own weight but may remain suspended for some time.

The tendency of a material to generate dust upon handling is known as its dustiness (Hamelmann and Schmidt, 2003). The exposure and deposition of airborne dust in various regions of the human respiratory tract depends on several factors including the size of the dust particle. Based on the size of a dust particle and its ability to penetrate and deposit in lungs, the three dust size fractions include the inhalable fraction (mouth/nose), the thoracic fraction (respiratory tract below the larynx) and the respirable fraction (the alveolar region in the lung) (Baron and Vincent, 1999; EN 481, 1993; ISO 7708, 1995). The size fractions depend on the aerodynamic diameter of the dust particles (Hinds, 1999) and are classified based on dust median particle size with 100 μm for inhalable, 10 μm for thoracic, and 4 μm for respirable fractions, for 50% sampling efficiency. The exposure to dust generated from the handling of silicon carbide powders in industries can lead to increased rates of chronic bronchopulmonary diseases and bronchial hyper-reactivity (Governa et al., 1997; Petran et al., 2000).

In an occupational setting, handling of materials including silicon carbide particles, may pose major challenges including the risk of inhalation of dust, changes in material quality, contamination of plant equipment, and in some cases, can even cause fire and explosion (Eckhoff, 2005). Dustiness of a powder depends on several factors including powder parameters such as particle size and particle morphology and external factors such as ambient humidity (Plinke, 1995). Testing for dustiness of a material involves measuring dust particles aerosolized from a specific amount of bulk material, subjected to a precise amount and type of energy for a defined period of time (Plinke et al., 1992). The time of suspension of a dust particle is directly related to its size, shape and density (Green, 2007; Klippel et al., 2013). Thus, it is important to not only test and report dustiness of HTF material (SiC) in their original pristine state but also at their used form in order to assess the risks of handling such material

and to select powders with suitable properties. The results could aid in quantifying and mitigating risks associated not only with planned activities such as handling and transportation of new and used HTF material but also with major incidents, such as an HTF leak in the plant. Thus measurement of the long-term dust generation of HTF powders is possibly as important as characterizing short-term dust generation (associated with activities such as the loading and unloading of powders) as the HTF powders continuously circulate in CSP plants for months without changing.

There are a wide range of dustiness testers including the air jet dispersion (Boundy et al., 2006) and gas fluidization systems (Saleh et al., 2014; Sethi and Schneider, 1996), drop test (Cowherd et al., 1989; Dahmann and Monz, 2011), the rotating drum (Breum, 1999; Schneider and Jensen, 2008). Among them, the latter two are the standard testers for measuring dustiness of bulk materials according to EN 15051 (EN, 2006). But these testers need large amounts of powders (35 cm³ or 500 g) (Morgeneyer et al., 2013; O'Shaughnessy et al., 2012) and can give disparate results for industrial minerals (Pensis et al., 2010). Hamelmann and Schmidt's (Hamelmann and Schmidt, 2004) review of several dustiness testers shows the lack of comparability between the testers due to differences in the bulk sample and generation techniques, and thus a single standardized test is not suitable for all powders and applications. Furthermore, most of the testers mentioned have only been used for short time durations (less than 1 hour) and may not be representative of the dust generated from processes with longer durations.

The vortex shaker (VS) method (Chakravarty et al., 2017a, 2017b; Le Bihan et al., 2014; Morgeneyer et al., 2013) is a promising dust generation method which is capable of functioning with very small sample quantities (less than 4g). (Morgeneyer et al., 2013) and (Le Bihan et al., 2014) used the VS method to test dust generation of micron-sized alumina particles and nanoscale carbon nano-tubes (CNTs) for one hour with sample mass as small as 0.5 g, respectively. (Morgeneyer et al., 2013) studied the minimum level of bulk mass and optimum vortex speeds necessary to aerosolize micron-sized alumina particles. They report a minimum sample mass of 2 g and a vortex speed of 1500 rpm - 1,800 rpm as suitable parameters for aerosolizing alumina particles without impacting the particle size distribution (PSD) of the powder. The VS setup also allows one to retrieve the used bulk sample after the end of the dustiness test for further analysis, but such results have not been reported in previous studies with the VS setup.

In this study, an experimental setup similar to (Morgeneyer et al., 2013) was used for testing the respirable dust generated by silicon carbide powders. Further, the tested powders were characterized for any change in PSD and shape properties due to testing. As HTFs in CSP plants are circulated for a prolonged duration, they require long-term monitoring of dust and change in powder properties. This study was focused on dust generation over six hours of vortex agitation for the worst case conditions, i.e., a dry filtered air flow and a vortex speed of 1500 rpm. This is a novel approach for studying dust generation in hard materials used for long-duration applications. Results from this study can support the selection process of an HTF

material and appraise the need for further dust generation monitoring with different test conditions.

The primary objective of this study is to test and evaluate the dust generation behavior of two samples of silicon carbide particles subjected to vortex rotation for six hours. The ultimate purpose is to gain insights into the physical mechanisms underlying dustiness and how various factors lead to differences in dust emission. The results of these studies can be used for material selection based on their dust generation behavior and change in physical properties over long periods of time.

The grain shape properties and size distributions of the bulk powders were compared for the tested and untested (pristine) bulk powder samples using laser diffraction and image analysis (described in the materials and methods section 2.3). Finally, hypotheses accounting for our observations were proposed along with recommendations regarding the choice of powders in such industrial operations.

2. Materials and Methods

2.1 Silicon carbide particles

Two sets of silicon carbide powders (CAS Number: 409-21-2), SiC F220 and SiC F320 (from Mineralex, France) were used "as-received" following the EN standard 15051 (CEN, 2006). The test samples consisted of 99% of silicon carbide obtained from high purity sand or quartz, fused in an oven with pet coke at temperatures above 2000 °C. The powder test samples were characterized for volumetric and number size distribution by laser diffraction (3D measurement) and image analysis (2D measurement), respectively. Also, the samples' specific surface area and water content were measured using the gas adsorption surface area analyzer (BET) and a halogen moisture analyzer, respectively. The material parameters are mentioned in Table 1.

F220 and F320 have the same particle density ($3,210 \text{ kg/m}^3$) and contain less than 0.1% of moisture by mass, measured before the dustiness test (

Table 11). The volumetric size distribution of the samples measured in wet mode shows F220 and F320 with normal size distribution, and F220 with a broader size distribution than F320 (**Error! Reference source not found.a**).

In order to compute number size distributions, the samples were prepared, dispersed automatically for measurement using the Morphologi G3s image analyzer (explained in section 2.3) according to the Malvern G3s user manual (*Morphologi G3 User Manual*, 2008). F220 shows a bi-modal size distribution with its first mode within the size bin of 0-5 μm in circle equivalent diameter (CED), i.e, the diameter of a circle with the same areas as the measured 2D image of the particle (**Error! Reference source not found.b**).

2.2 Vortex shaker dustiness tester

The VS setup was used as the dustiness tester due to its low requirements of sample sizes, ease of operation and the ability to retain the powder sample after the test. The experimental setup used by (Chakravarty et al., 2017b; Jensen, 2012) was adopted for the present study. The setup broadly consists of 4 sections; generation, sampling, dilution, and measurement (**Error! Reference source not found.**).

For aerosol generation, a powder-filled centrifuge test-tube (made of glass) was mounted on a digital vortex shaker (VWR Signature Digital Vortex Mixer). The shaker which is capable of achieving constant rotational speeds, was set to rotate at 1500 rpm along the vertical axis. The centrifuge tubes were sealed using a rubber stopper with provisions for an inlet to channel HEPA filtered dry air (at 4.2 L/min or $7\text{e-}05\text{ m}^3/\text{s}$) and an outlet to emit air containing aerosolized particles (also at 4.2 L/min).

Airborne dust particles were sampled using a BGI GK 2.69 cyclone operated at a volumetric flow rate of 4.2 L/min ($7\text{e-}05\text{ m}^3/\text{s}$) to meet the requirements of sampling for respirable size fraction (Jensen, 2012). The respirable fraction of aerosol released is then diluted with 7.4 L/min ($1.2\text{e-}04\text{ m}^3/\text{s}$) of filtered air (HEPA) and split into 3 channels for measurement and characterization. Particles with size larger than the respirable size fraction fall into the grit pot and are discarded. The flow through the sampler was checked and calibrated before starting each experiment.

The aerosol concentration of the respirable dust is measured at different bin size ranges using an aerodynamic particle sizer (APS TSI 3321, TSI Inc., Shoreview, MN). The APS records the particle counts by their aerodynamic size measured based on the time-of-flight of individual aerosol particles. It measured the aerosol number concentration over 51 size channels from $0.54\text{ }\mu\text{m}$ to $20\text{ }\mu\text{m}$, recorded every 5 sec with a total flow rate of 5 L/min. Furthermore, it calculates the mass of individual spherical particles for a given particle density (TSI, APS Application notes). Since the minimum APS size detection limit inhibits its ability to quantify all particles in the respirable range ($<4\text{ }\mu\text{m}$), a condensation particle counter (CPC TSI 3775, TSI Inc., Shoreview, MN) is used to measure the concentration of aerosol particles with size ranging from $0.004\text{ }\mu\text{m}$ to $3\text{ }\mu\text{m}$. The CPC measurements span over a wide concentration ranging from 0 to 10^7 particles or $\#/\text{cm}^3$ with high accuracy. An aerosol particle sampler, the Mini-Particle-Sampler (MPS®) (R'mili et al., 2013) was used to capture and deposit aerosol particles on copper grids for off-site transmission electron microscope (TEM) analysis.

Measures to minimize electrostatic charging during the transportation of dust included grounding the conductive aerosol outlet tube (stainless) and silicone tubes (diameter, $4.8\text{e-}03\text{ m}$) especially designed for particle transport (TSI Inc., USA). The total length of tubes

connecting the aerosol source to the measurement devices was reduced to 0.9 m as compared to 1.2 m used by (Morgeneyer et al., 2013) to minimize the settling of dust particles in tubes. For ensuring safety while conducting the dustiness tests, all the experimental equipment were installed and operated inside a state-of-the-art closed isolator system at the Nanosecured (S-NANO) platform at the INERIS in Verneuil-en-Halatte, France. A more detailed description of the setup and powder handling process has been reported in (Le Bihan et al., 2014; Morgeneyer et al., 2013) dealing with the aerosolization of micron-size alumina and nano-sized carbon nanotubes, respectively.

2.3 Optical microscopy and particle morphology

Particles from powder samples, F220 and F320 were quantitatively characterized with respect to their size and morphology using dry dispersion of powder in the particle image analyzer (Morphologi G3S, Malvern, UK) *before and after* the dustiness test. The particles were measured at a magnification of 20x with a 5-megapixel CCD camera to enable the digital analysis of particles shapes.

The analysis captures a 2D image of a 3D particle and calculates various size and shape parameters of the 2D image such as the circle equivalent diameter (CED), high sensitivity circularity (HSC) and convexity. CED is the diameter of the circle with the same surface area as the projected area of the particle. HSC values indicate the degree of roundness of the particles when compared to a perfect circle. It is calculated using the equation,

$$\text{HSC} = (4\pi \times A)/P^2 \quad \text{Eq. (1)}$$

Where, A and P are the projected area and the perimeter, respectively. A perfect circle has an HSC value of 1 whereas an irregularly shaped object has a value closer to 0. Further, convexity is the measure of surface roughness in a particle, calculated as the ratio of “convex hull perimeter” by the actual perimeter of a particle (*Morphologi G3 User Manual*, 2008). A smoothly shaped particle has a convexity of 1 whereas a “spiky” or irregularly shaped particle has a value closer to 0. Aspect ratio (AR) is the ratio of the width to the length of the particle, where the width and length of the particle is the longest length of the projected particle on the major and minor axis, respectively.

2.4 Test protocol

Three trials were performed for each of the two powders, F220 and F320. Each test used 2 g of powder weighed with an accuracy of ± 0.001 g using an analytical balance (MS1003S, Mettler-Toledo, Inc., Columbus, OH, USA), manually filled in a centrifuge glass tube (diameter 0.025 m, height 0.15 m). The filled tube was sealed using a rubber stopper and

carried to the isolator system. The powders were weighed within 1 hour of performing the experiments to limit the number of variables affecting the experimental condition.

The sample filled centrifuge tube was then mounted on the VS using a rubber cup to hold the tube firmly. Prior to starting the vortex shaker, the APS and CPC sampling were turned on along with the inlet flow (4.2 L/min or 7×10^{-5} m³/s) and dilution flow (7.4 L/min or 1.2×10^{-4} m³/s) for 2 minutes. Opening the inlet flow shows a peak in the particle concentration (close to 10 particles/cm³) which rapidly decreases to the background values, usually lower than the detection limit of the APS (0.1 particles/cm³) and CPC (0.2 particles/cm³).

Thus the inlet air flow is only used to transport the aerosol generated through the vortex motion and does not influence the generation of dust particles in the system.

The VS operated at 1500 rpm, was run for six hours to test the powder samples, with a short break of 5 minutes after every 1-hour interval to avoid the overheating of the electric motor. Since the air flow is not interrupted, the peaks in the dustiness variables are entirely due to the mechanical action of the vortex shaker. The measured values begin and end 2 minutes before and after the vortex shaker running time, respectively. Each test was analyzed as an individual case. Using a low-pressure pump (0.6 L/min or 1×10^{-5} m³/s, Gilian LFS-113DC) attached to the sampler (MPS®), dust particles were collected on Quantifoil copper-carbon grids (Oxford Instruments, UK) (R'mili et al., 2013). The dust particles confined in these grids were further analyzed for their morphology using a Transmission electron microscope (TEM, JEOL JEM-2100F, operated at 100 kV).

Calculation

Total respirable particle number concentrations measured for different particle size ranges from CPC (0.004 μm to 3 μm) and APS (3 μm to 19.5 μm) were combined to calculate the total number of generated particles, $S_{Vortex}^{Number (Total)}$ using Eq. (2) to (4), modified from (Jensen, 2012).

$$S_{Vortex}^{Number (CPC)} = [Q_{Vortex} + Q_{Dilution}] \times \Delta t_{CPC} \times \sum_{i=0}^{T/\Delta t_{CPC}} C_{n,CPC}(t_0 + i \times \Delta t_{CPC}) \quad \text{Eq. (2)}$$

$$S_{Vortex}^{Number (APS)} = [Q_{Vortex} + Q_{Dilution}] \times \Delta t_{APS} \times \sum_{i=0}^{T/\Delta t_{APS}} C_{n,APS}(t_0 + i \times \Delta t_{APS}) \quad \text{Eq. (3)}$$

$$S_{Vortex}^{Number (Total)} = S_{Vortex}^{Number (CPC)} + S_{Vortex}^{Number (APS)} \quad \text{Eq. (4)}$$

where Q_{Vortex} and $Q_{Dilution}$ are the flow rates for the filtered air directed towards the vortex tube (7×10^{-5} m³/s) and for dilution (1.2×10^{-4} m³/s), respectively. T is the time of the test for which the aerosol particles are calculated (6 intervals of 3,600 seconds). Δt_{CPC} (1s) and Δt_{APS} (5s) are the time-step set for the CPC and the APS, respectively. $C_{n,CPC}(t_0 + i \cdot \Delta t_{CPC})$ and $C_{n,APS}(t_0 + i \cdot \Delta t_{APS})$ are the aerosol number concentrations (in particles/cm³) for the ith time interval measured by the CPC and the APS, respectively.

Additionally, APS number concentrations ($C_{n,APS}$, in particles/cm³) were used to calculate the volume of the assumed spherical particles, which is then transformed to mass concentration ($C_{m,APS}$, in mg/m³) for each size channel adjusted for the particle density of the SiC particle, ρ_p (3,210 kg/m³) using Eq. (5). The APS software uses a pre-installed algorithm for Stokes correction reported by (Wang and John, 1987).

$$C_{m,APS} = \rho_p V_{APS} = \rho_p \times \sum_l^u \left[\frac{\pi}{6} \left(D_a \sqrt{\frac{\rho_0}{\rho_p}} \right)^3 \times C_{n,APS} \right] \quad \text{Eq. (5)}$$

where V_{APS} is the total volume concentration ($\mu\text{m}^3/\text{cm}^3$), D_a is the aerodynamic diameter of the particle and ρ_0 is the unit density (1 g/cm³ or 1000 kg/m³). The total mass of the respirable fraction of particles, M_{Vortex}^{APS} is then calculated using Eq. (6),

$$M_{Vortex}^{APS} = [Q_{Vortex} + Q_{Dilution}] \times \Delta t_{APS} \times \sum_{i=0}^{T/\Delta t_{APS}} C_{m,APS}(t_0 + i \times \Delta t_{APS}) \quad \text{Eq. (6)}$$

Furthermore, number and mass based dustiness indices (DI) were calculated for the dust generated per unit mass of powder, using Eq. (7) and (8)

$$DI_{number} \left(\frac{1}{\text{mg}} \right) = S_{Vortex}^{Number (Total)} / m \text{ (in mg)} \quad \text{Eq. (7)}$$

$$DI_{mass} \left(\frac{\text{mg}}{\text{kg}} \right) = M_{Vortex}^{APS} \text{ (in mg)} / m \text{ (in kg)} \quad \text{Eq. (8)}$$

Whereby, m stands for the mass of the test sample.

3. Results

3.1 Respirable dustiness measurements

3.1.1 Evolution of aerosol release

The standard deviations of the dustiness variables (particle count, aerosol mode size) are generally smaller than the differences between the averaged values for the two powders. It thus appears to be a statistically significant difference regarding the behavior of the two agitated powders that needs to be accounted for. In general, both samples (F220 and F320) release respirable fractions of aerosol but their dust generation behavior differs (**Error! Reference source not found.** bottom). During the six-hour test, the aerosol mode particle size by mass (**Error! Reference source not found.** top) for F220 shows a greater deviation towards smaller particle sizes compared to the F320 sample.

Aerosol generated from F220 and F320 can be classified into four stages based on the evolution of the total respirable aerosol counts (**Error! Reference source not found.**).

Stages IV-IV:

Stage I (Rapid Emission): At the onset of the VS, F220 rapidly emits aerosol with the maximum number of aerosol released (approximately 5 to $7e+06$) within the 20th minute of the test duration. F320 shows a similar behavior but with an aerosol count about 2-3 times lower than F220. Furthermore, the mode aerosol size measured for F220 and F320 using the APS shows similar values at the start of the experiment (**Error! Reference source not found.** top).

Stage II (Reduction): From its maximum at the 0-20th minute interval, the F220 and F320 aerosol numbers decrease to some local minima ($2.7e+06$ for SiC F220 and $1.1e+06$ for SiC F320) within the 160th - 180th minute-intervals of the test.

Stage III (Steady generation and release-1): Aerosol released from F320 are relatively stable from the 180th minute to the 300th minute, but F220 shows a slight increase in particle emission compared to F320 with some variation in the aerosol release measured by the CPC and APS, combined.

Stage IV (Slow generation): From the 300th minute till the end of the vortex shaker test, aerosol counts for F220 gradually increases by 14% as compared to a decrease of 42% for F320, for the same time interval.

3.1.2 Aerosol size distribution

Aerosol mode particle size ($D_{p,mode}$) (shown in **Error! Reference source not found.** (top) was used as an indicator of change in aerosol size distribution with vortex time duration. Cumulative aerosol mass concentration ($\sum_{i=0}^{T/\Delta t_{APS}} C_{m,APS}(t_0 + i \cdot \Delta t_{APS})$) from the APS, split in 20-minute time intervals were grouped and analyzed for change in aerosol mode particle size ($D_{p,mode}$). For the APS size range of $0.5 \mu\text{m}$ to $19.5 \mu\text{m}$, the average $D_{p,mode}$ released by F320 lies within a stable range of $2.2 \mu\text{m}$ to $2.3 \mu\text{m}$ whereas aerosol from F220 shows a slightly wider size range of $1.5 \mu\text{m}$ and $2.3 \mu\text{m}$ for the six hours of testing.

3.1.3 Number dustiness index

Respirable number dustiness indices for samples F220 ($DI_{n,F220}$) and F320 ($DI_{n,F320}$) are calculated from real-time aerosol concentration from the CPC and the APS using Eq. (7). For F220, $DI_{n,F220}$ ($7098/\text{mg}$) at the 1st hour of vortex decreases by 27% and 21% by the 2nd and 3rd hour-intervals, respectively, followed by an increase of 14%, 10%, 12% in the 4th to 6th hour-intervals (**Error! Reference source not found.**). As for F320, $DI_{n,F320}$ in

the 1st hour (3455/mg) decreases by 29%, 28%, 5%, 9% and 6% in the progressing 2nd, 3rd, 4th, 5th and 6th hour-intervals. Thus, both the micron-scale powders show DI_n in the range of $1E+03$ to $1E+04$, which are typically one to two orders of magnitude lower than the VS dustiness tests using nano-powders for different time durations (Dazon et al., 2017; Jensen, 2012). Furthermore, the increasing trend of DI_n (measured by APS and CPC) after 3 hours for SiC F220 is different from the stable profile of DI_{mass} (measured by APS, **Error! Reference source not found.**) for the same time means the increasing trend is due to the emission of finer particles lower than the measurement range of the APS.

A parabolic fit for F220 (Eq. 9) and a power law fit for F320 (Eq. 10) can provide a reasonable approximation to the average respirable number dustiness over the 6-hour test duration.

$$DI_{n,F220} = 1168 (t_h^2) - 323 (t_h) + 4373 \quad \text{Eq. (9)}$$

$$DI_{n,F320} = 3457 (t_h)^{-0.53} \quad \text{Eq. (10)}$$

3.1.4 Mass dustiness index

Respirable mass dustiness indices for F220 ($DI_{m,F220}$) and F320 ($DI_{m,F320}$) are calculated using Eq. (8) based on the APS measurements. Similar to DI_n (**Error! Reference source not found.**), $DI_{m,F220}$ and $DI_{m,F320}$ show maximum values at the start of the test (**Error! Reference source not found.**). With time, while both $DI_{m,F220}$ and $DI_{m,F320}$ decreases, $DI_{m,F220}$ shows an increase of 16% from the 3rd to the 6th hour of the test duration. The average DI_m values for F220 and F320 are fitted to a quadratic (Eq. 11) and power law (Eq. 12) expressions, respectively. Compared to the VS tests with nano-powders (Dazon et al., 2017; Jensen, 2012), the DI_m values for the F220 and 320 powders are around one order magnitude lower.

$$DI_{m,F220} = 750 (t_h^2) - 6412 (t_h) + 17310 \quad \text{Eq. (11)}$$

$$DI_{m,F320} = 5643 (t_h)^{-0.70} \quad \text{Eq. (12)}$$

3.1.5 TEM micrographs

Examining approximately 50 photomicrographs from each sample (F220 and F320) shows a wide range of sizes and shapes of the respirable aerosol particles generated from the

F220 and F320 samples. The aerosol particles sampled between the 350th and the 360th minute (**Error! Reference source not found.**: c, d, g, h) show angular shaped particles with at least one smooth surface (marked with a dotted line) with fewer surface asperities compared to the aerosols with rugged surfaces sampled between the 25th to 30th minute interval (**Error! Reference source not found.**: a, b, e, f).

3.2 Characterization of the tested powder samples

3.2.1 Size distribution of the powder

Volumetric size distribution

After 6-hours of VS operation, the tested powder samples were characterized with respect to changes in their PSD by volume using a laser diffraction particle size analyzer (**Error! Reference source not found.**a and Table 2.). The testing of the F320 sample (F320_tested) shows negligible change in its size distribution compared to the pristine samples (F320). The differences with respect to volumetric x_{10} , x_{50} and x_{90} of the powder range from 0.6, 0.3 and -0.3 , respectively which are close or inferior to the standard deviation stemming from the four repeated trials.

On the other hand, the tested F220 sample (F220_tested) shows noticeable changes in powder PSD where volumetric x_{90} and x_{50} decreases by 6, and 1.7, respectively although x_{10} increases by 1.1. Those changes are significantly higher than the standard deviations for the 4 repeated trials.

Number size distribution

Circle Equivalent Diameters (CED) of individual grains from fresh (F220 and F320) and tested (F220_tested and F320_tested) samples were measured using image analysis. A minimum of 30,000 particles were analyzed for each of the 3 trials per sample. Similar to the volume size distribution (Table 2.), F320 samples shows negligible changes in PSD for the pristine and tested powders whereas the F220 shows a distinguishable change in PSD from its pristine to tested state.

The tested samples for both SiC F220 and SiC F320 powders show an increase in the population of particles with sizes less than 20 μ m, indicating the availability of aerosolizable fine particles even after 6 hours of testing (**Error! Reference source not found.**b). In comparison to their pristine samples, the tested F320 samples show a slight increase in the

number of particles less than 20 μm , whereas tested F220 shows about 20% increase for the particular size range.

3.2.2 Change in particle morphology

The Morphologi G3s analyzer was used for static image analysis and corresponding measurement of particle shape properties including high sensitivity (HS) circularity, convexity and aspect ratio (AR). The principles it relies on are laid out in section 2.3. The measured average values of HS circularity (0.81) and AR (0.73) for SiC F320 were 16% and 18% greater than the larger sized SiC F220 particles, shows the F320 particles as more circular in shape compared to SiC F220 (see Table 3). Also, there were almost no differences in the average convexity for both the powders, thus indicating no detectable ‘spikiness’ or roughness in in the particle shape.

Compared to the measurements from the pristine samples, F320_tested shows no change in mean HS circularity or aspect ratio (Table 3.). But, tested samples of F220 (F220_tested) shows a 6% increase in both HS circularity and aspect ratio, respectively (Table 3).

While F320 particles shows mostly circular particles with a Gaussian-like distribution over particle sizes 5-50 μm (Fig. 8c and 8d), there are few changes observed in the distribution of F220 particles over circularity and particle size (Fig. 8a and 8b). The fine particles (close to 0-10 μm) for the tested particles show a wide range of HS circularity from 0.2 to 1. Also, the tested F220 particles show a decrease in the proportion of particles within the sizes of 15 μm - 50 μm and an increase in particles (with relatively greater circularity) with sizes 50 μm - 100 μm , as compared to the F220 pristine.

4. Discussion

4.1 Aerosol measurement

The combination of APS and CPC was found suitable for determining the respirable dustiness by number and mass, for micron-sized F220 and F320. A powder mass of 2 g and a vortex speed of 1500 rpm were enough to measure the respirable aerosols within the lower and upper bounds of the APS and the CPC, similarly to the study of dustiness in alumina particles (Morgeneyer et al., 2013).

The number and mass dustiness indices of powders can be used to compare dustiness from different powder samples (Jensen, 2012). The ratio of DI_n for SiC F220 and F320 shows a progressive increase from 2.1 to 5.1 during the experiment, whereas the ratio of DI_m decreases from 2.2 (1st hour) to 1.6 (2nd hour), before reaching its maximum value 3.7 in the 6th and final 1-hour interval. We postulate that the disparity in the trends of hourly numbers and mass dustiness indices for SiC F220 measured using the CPC and APS, respectively (**Error! Reference source not found.** and **Error! Reference source not found.**) may stem from the difference in the aerosol size ranges measured by the CPC (0.004 μm to 3 μm) and the APS (3 μm to 19.5 μm). Dust released in the initial hour is a combination of coarser and fine particles but with time, there is reduction in dust emission for both powders but the SiC F220 shows an increase in small fine-scale dust particles, unlike the SiC F320 samples. These fine-scale aerosols (whose sizes are smaller than 0.5 μm) are counted by the CPC and can be seen in TEM micrographs (**Error! Reference source not found.c** and **Error! Reference source not found.d**). Furthermore, the mass of the sub-micron sized aerosol particles with sizes lower than the APS detection limit ($d_{ae} < 0.5 \mu\text{m}$) has little contribution to the total mass measured (O'Shaughnessy et al., 2012)

The TEM micrographs for F220 and F320 show aerosol particles with at least one smooth edge (marked by a dotted line in **Error! Reference source not found.c**, **Error! Reference source not found.d**, **Error! Reference source not found.g**, **Error! Reference source not found.h**). The smooth surface of the aerosol particles can be due to the chipping of small angular fragments from the original SiC particles. An analysis of the aerosol shapes and sizes between the 1st and the 6th hour could further improve our understanding of the evolution of the aerosol particles generated from F220 and F320.

4.2 Dustiness due to particle attrition

F220 and F320 undergo mechanical stresses due to inter-particle collisions and particle-wall impacts in the VS. Although hard materials like SiC particles are resistant to breakage or fragmentation, they can undergo attrition due to abrasion or combination of fragmentation and abrasion, depending on the stresses they are subjected to (Ness and Zibbell, 1996; Quercia et al., 2001). Generally, the abrasion of particles leads to the rounding of the primary mother particles by reducing surface asperities resulting in the generation of fine-scale particles, thus creating a bi-modal number size distribution without any significant changes in the PSD by volume (Yang, 2003).

Based on the present results of the dustiness tests of SiC particles, the initial dust generation strongly depends on the population size of the aerosolizable particles present in the bulk material. The abrasion of larger particles generates fine aerosolizable particles and is a crucial part of the overall dust generation mechanism. The dust generation mechanism can be broadly divided into two stages (**Error! Reference source not found.**):

A: direct release of aerosolizable primary particles,
B: release of aerosolizable fines generated through the attrition of larger primary particles.

While the volumetric PSD does not show particles in the respirable size range (**Error! Reference source not found.a, Error! Reference source not found.a**) with respect to F220 and F320, the number PSD for both F220 and F320 show bi-modal size distributions revealing the presence of particles with CED smaller than 10 μm (**Error! Reference source not found.b, Error! Reference source not found.b**). Such fine-scale particles already present in the bulk samples can contribute to the initial release of respirable aerosol for F220 and F320 (**Error! Reference source not found.**). With 32% of particles with CED smaller than 10 μm , F220 generates 2.3 times more respirable aerosol particles in the initial 20 minutes of the vortex shaker test (Stage I, **Error! Reference source not found.**) compared to F320 consisting of less than 6% of particles smaller than 10 μm .

Stage II can be considered as the relatively gradual reduction in dust emission after the peak of dust emission (Stage I) shown by both SiC F220 and F320 powders. The end of Stage II lies at the 160th - 180th minute-interval for both powders (**Error! Reference source not found.**), where the respirable aerosol counts for F220 and F320 reaches their respective local minima, which indicates diminished reserves of aerosolizable dust particle for both SiC powders.

In stage III, the respirable aerosol counts for both F220 and F320 levels off to a relative steady-state (180th to 300th minute, **Error! Reference source not found.**). One possible interpretation of this stage may be that the rate of generation of respirable aerosols in the bulk equals the rate of aerosols released from the bulk. In comparison to the smaller sized SiC F320 particles, F220 powder shows an increasing tendency to release dust, i.e., an increase in generation of respirable aerosols with time. The increase in fine production allows SiC 220 to maintain a reservoir of fine-scale aerosolizable particles (with CED up to 10 μm) thus showing an increase in the population of particles with sizes smaller than 10 μm . The coarser particles in F220 (CED up to 125 μm) are particularly prone to attrition due to abrasion as they tend to contain more faults in the form of microcracks or imperfections and a higher surface area for particle-wall interactions compared to smaller sized particles present in SiC F320.

In Stage IV there is an observable change in the powder emission behavior for both powders. F320 emissions decreases by 42% till the end of the 6-hour test duration. The decrease in F320 aerosol counts with time (**Error! Reference source not found.**) suggests a diminishing number of fines generated from attrition, that is to say, the F320 particles resist attrition and thus limits the production and generation of fine-scale respirable dust. The smaller, more attrition resistant SiC F320 shows hardly any change in PSD by number or volume due to the 6 hours of vortex shaker test.

Contrarily to SiC F320 powders, F220 emissions increase by 14%. Characterization of the tested F220 powders show a decrease in median particle size (x_{50}) of 49% and 2.5% based on the number (**Error! Reference source not found.**b, Table 3.) and volume (**Error! Reference source not found.**a, Table 2.) size distributions, respectively. The aerosolization of fine-scale particles from a specific quantity of particles present in the bulk can lead to an increase in x_{10} due to the absence of the aerosolized particles at the end of the vortex test (PSD by volume shown in **Error! Reference source not found.**a, Table 2.). Further, a decrease in x_{90} suggests a reduction in the size of large-sized particles, potentially due to the attrition of small fragments from the larger particles inside the VS system.

Results from the image analysis of the particle shape properties show SiC F320 particles as relatively more circular in shape with higher average aspect ratio compared to the larger SiC F220 particles. The F220 tested particles show small increases in particle HS circularity and aspect ratio compared to almost no change measured for the tested and pristine SiC F320 particles. The relatively larger and sharply shaped fresh F220 particles show inclination towards becoming rounder (increasing HSC and AR in F220_tested) by shedding angular corners in collisions (**Error! Reference source not found.**a, Table 3.). This phenomena has been reported for other particles such as sodium benzoate with increasing particle impaction (Laarhoven et al., 2012). On the contrary, the less dusty F320 particles are smaller in size and retains its circularity and aspect ratio during the 6 hours of vortex. There are indications in the literature that circular particles are more resistant to attrition than non-circular ones (Laarhoven et al., 2012; Van Laarhoven, 2010). This might account for the fact that primary particles from F320 that have more circular shapes generate less fines than primary particles from F220 which have an irregular shape while there are no discernable changes particle surface roughness (convexity values in Table 3.)

5. Conclusion and Perspective

Particles used for applications extending over a long period of time, such as HTFs in CSP solar thermal plants require results from sufficiently long dustiness tests to support the selection of material and quantify the risk associated with the handling of new and used particles. In this case study, we investigate dust release over six hours for two potential silicon carbide HTFs (F220 with x_{50} by volume = 68 μm and F320 with x_{50} by volume = 38 μm) using the VS method.

Test results show the release of the respirable fraction of dust particles from both samples, but F220 is found to be more prone to generate dust than F320. The hourly dustiness index (by number) ratio of F220 and F320 increases from 2.1 in the 1st hour to 5.1 at the 6th hour. For F320, an initial rise in the aerosol release is followed by a gradual decrease with time, following a power law distribution. Unlike F320, aerosol generation and release from F220 is more complex and the dust released over time shows a quadratic fit.

F220 and F320 not only differ in dustiness but also in the mechanism of dust generation and release. Two dust generation mechanisms are proposed which can potentially explain the dustiness behavior of F220 and F320 over a 6-hour duration. Results from the dustiness measurement, TEM micrographs of the aerosol particles and characterization of pristine and tested

powder samples by their size and shape suggest that the dust generation from F220 and F320 is related to the presence of aerosolizable fine-scale particles already present in the bulk as well as the particles generated from powder attrition.

The tested F220 powders show changes in particle size distribution and shape properties compared to their pristine form, indicating abrasion as the dominant source of attrition. On the contrary, the F320 powders show barely any changes in particle size distribution or shape factors with vortex testing.

Understanding the difference of aerosol generation behavior based on particle shape requires further work and the effect should be more observable for materials softer and more fragile than SiC. F220 and F320 bulk samples could be further characterized by their particle size distribution and shape properties for every hour to analyze the evolution of particle properties with dust generation. The handling of F220 (SiC 220) may generate fine-scale particles which may affect the safe and efficient operation of SiC HTFs in CSP plants. Our study underlines the importance of characterizing both before and after the dustiness test, as changes in its properties are crucial to understand the underlying dust generation mechanisms.

In the industrial world, powders which have already undergone an *ageing process* for several weeks or months are employed in the CSP plants. Studying such aged powders with respect to their dust generation behavior appears worthwhile. The fact that the dustiness of powder F320 diminishes with time might make it potentially more interesting for industrial applications compared to its counterpart F220 whose dustiness index ends up increasing with time. Further studies are necessary to investigate its potential greater suitability for long-term uses.

6. Acknowledgement

This work was supported by the EU's FP7 Marie Curie ITN T-MAPPP under the grant agreement no ITN607453, Région Picardie/Hauts de France and by the Programme 190 (French Ministry of Environment). This study was performed in the framework of the CSP2 Project (Concentrated Solar Power in Particles), funded by the European Commission (FP7, Project No. 282 932).

We thank François Oudet (UTC) for the TEM images, Michaël Lefebvre, Bruno Dauzat and Hervé Leclerc from UTC, France for the particle characterization and Arunima Murgai for critically reading this manuscript.

References

- Baron, P., Vincent, J., 1999. Particle size-selective sampling of particulate air contaminants.
- Benoit, H., Pérez López, I., Gauthier, D., Sans, J.-L., Flamant, G., 2015. On-sun demonstration of a 750°C heat transfer fluid for concentrating solar systems: Dense particle suspension in tube. *Sol. Energy* 118, 622-633. <https://doi.org/10.1016/j.solener.2015.06.007>
- Boundy, M., Leith, D., Polton, T., 2006. Method to Evaluate the Dustiness of Pharmaceutical Powders 50, 453-458. <https://doi.org/10.1093/annhyg/mel004>
- Breum, N.O., 1999. The Rotating Drum Dustiness Tester : Variability in Dustiness in Relation to Sample Mass , Testing Time , and Surface Adhesion 43, 557-566. [https://doi.org/http://dx.doi.org/10.1016/S0003-4878\(99\)00049-6](https://doi.org/http://dx.doi.org/10.1016/S0003-4878(99)00049-6)
- Chakravarty, S., Fischer, M., García-Triñanes, P., García-Triñanes, P., Parker, D., Le Bihan, O., Morgeneyer, M., García-Triñanes, P., Parker, D., Bihan, O.L.O. Le, Morgeneyer, M., 2017a. Study of the particle motion induced by a vortex shaker. *Powder Technol.* 322, 54-64. <https://doi.org/10.1016/j.powtec.2017.08.026>
- Chakravarty, S., Le Bihan, O., Fischer, M., Morgeneyer, M., 2017b. Dust generation in powders: Effect of particle size distribution, in: *EPJ Web of Conferences*. EDP Sciences, p. 13018. <https://doi.org/10.1051/epjconf/201714013018>
- Cowherd, C., Grelinger, M.A., Englehart, P.J., Kent, R.F., Wong, K.F., 1989. An apparatus and methodology for predicting the dustiness of materials. *Am. Ind. Hyg. Assoc. J.* 50, 123-130.
- Dahmann, D., Monz, C., 2011. Determination of dustiness of nanostructured materials. *Gefahrstoffe - Reinhaltung der Luft* 71, 481-487.
- Dazon, C., Witschger, O., Bau, S., Payet, R., Beugnon, K., Petit, G., Garin, T., Martinon, L., 2017. Dustiness of 14 carbon nanotubes using the vortex shaker method. *J. Phys. Conf. Ser.* 838. <https://doi.org/10.1088/1742-6596/838/1/012005>
- Eckhoff, R., 2005. Current status and expected future trends in dust explosion research. *J. loss Prev. Process Ind.*
- EN, C., 2006. EN 15051 Workplace atmospheres—measurement of the dustiness of bulk materials—requirements and test methods. Brussels, Belgium Eur. Comm. Stand.
- EN, C., 1993. 481 Workplace atmospheres: specification for conventions for measurement of suspended matter in workplace atmospheres. Brussels, Belgium Eur. Comm.
- García-Triñanes, P., Seville, J., Boissière, B., 2016. Hydrodynamics and particle motion in upward flowing dense particle suspensions: Application in solar receivers. *Chem. Eng.*
- Governa, M., Valentino, M., Amati, M., Visonà, I., Botta, G.C., Marcer, G., Gemignani, C., 1997. Biological effects of contaminated silicon carbide particles from a workstation in a plant producing abrasives. *Toxicol. Vit.* 11, 201-207. [https://doi.org/10.1016/S0887-2333\(97\)00018-0](https://doi.org/10.1016/S0887-2333(97)00018-0)

- Green, D.W., 2007. Perry's chemical engineering handbook. McGrawHill Prof.
- Hamelmann, F., Schmidt, E., 2004. Methods for characterizing the dustiness estimation of powders. *Chem. Eng. Technol.* 27, 844-847. <https://doi.org/http://dx.doi.org/10.1002/ceat.200403210>
- Hamelmann, F., Schmidt, E., 2003. Methods of Estimating the Dustiness of Industrial Powders - A Review. *KONA Powder Part. J.* 21, 7-18. <https://doi.org/10.14356/kona.2003006>
- Harris, G., 1995. Properties of silicon carbide. Institution of Engineering and Technology.
- Hinds, W.C., 1999. Aerosol technology: Properties, Behavior, and Measurement of Airborne Particles., Wiley-Interscience Publication. [https://doi.org/10.1016/0021-8502\(83\)90049-6](https://doi.org/10.1016/0021-8502(83)90049-6)
- International Organization for Standardization, 1995. ISO 7708: Air quality—particle size fraction definitions for health-related sampling. Geneva, Switzerland: International Organization for Standardization.
- International Organization for Standardization, 1994. ISO 4225: Air quality - General aspects - Vocabulary.
- Jensen, K.A., 2012. Towards a method for detecting the potential genotoxicity of nanomaterials. D4.6: Dustiness of NANOGENOTOX nanomaterials using the NRCWE small rotating drum and the INRS Vortex shaker. Copenhagen, DENMARK.
- Klippel, A., Scheid, M., Krause, U., 2013. Investigations into the influence of dustiness on dust explosions. *J. Loss Prev. Process.*
- Laarhoven, B. van, Schaafsma, S., Meesters, G.M.H., 2012. Toward a desktop attrition tester; validation with dilute phase pneumatic conveying. *Chem. Eng. Sci.* 73, 321-328.
- Le Bihan, O.L.C., Ustache, A., Bernard, D., Aguerre-Chariol, O., Morgeneyer, M., 2014. Experimental Study of the Aerosolization from a Carbon Nanotube Bulk by a Vortex Shaker. *J. Nanomater.* 2014, 1-11. <https://doi.org/10.1155/2014/193154>
- Morgeneyer, M., Le Bihan, O., Ustache, A., Aguerre-Chariol, O., 2013. Experimental study of the aerosolization of fine alumina particles from bulk by a vortex shaker. *Powder Technol.* 246, 583-589. <https://doi.org/10.1016/j.powtec.2013.05.040>
- Morphologi G3 User Manual, MAN0410 Is. ed, 2008. . Malvern Instruments Ltd. United Kingdom.
- Ness, E., Zibbell, R., 1996. Abrasion and erosion of hard materials related to wear in the abrasive waterjet. *Wear* 196, 120-125. [https://doi.org/10.1016/0043-1648\(95\)06886-4](https://doi.org/10.1016/0043-1648(95)06886-4)
- O'Shaughnessy, P.T., Kang, M., Ellickson, D., 2012. A Novel Device for Measuring Respirable Dustiness Using Low-Mass Powder Samples. *J. Occup. Environ. Hyg.* <https://doi.org/10.1080/15459624.2011.652061>
- Pensis, I., Mareels, J., Dahmann, D., Mark, D., 2010. Comparative evaluation of the dustiness of industrial minerals according to European standard en 15051, 2006. *Ann. Occup. Hyg.* 54, 204-216. <https://doi.org/10.1093/annhyg/mep077>

- Petran, M., Cocarla, A., Baiescu, M., 2000. Association between Bronchial Hyper-reactivity and Exposure to Silicon Carbide. *Occup. Med. (Chic. Ill)*. 50, 103-106. <https://doi.org/10.1093/occmed/50.2.103>
- Plinke, M.A.E., 1995. Dust generation from handling powders in industry. *Am. Ind. Hyg. Assoc. J.*
- Plinke, M., Maus, R., Leith, D., 1992. Experimental examination of factors that affect dust generation by using Heubach and MRI testers. *Am. Ind. Hyg.*
- Quercia, G., Grigorescu, I., Contreras, H., 2001. Friction and wear behavior of several hard materials. *Hard Mater.*
- R'mili, B., Le Bihan, O.L.C., Dutouquet, C., Aguerre-Charriol, O., Frejafon, E., 2013. Particle Sampling by TEM Grid Filtration. *Aerosol Sci. Technol.* 47, 767-775. <https://doi.org/10.1080/02786826.2013.789478>
- Saleh, K., Moufarej Abou Jaoude, M.T., Morgeneyer, M., Lefrancois, E., Le Bihan, O., Bouillard, J., 2014. Dust generation from powders: A characterization test based on stirred fluidization. *Powder Technol.* 255, 141-148. <https://doi.org/10.1016/j.powtec.2013.10.051>
- Schneider, T., Jensen, K.A., 2008. Combined Single-Drop and Rotating Drum Dustiness Test of Fine to Nanosize Powders Using a Small Drum. *Ann. Occup. Hyg.* 52, 23-34. <https://doi.org/10.1093/annhyg/mem059>
- Sethi, S.A., Schneider, T., 1996. A gas fluidization dustiness tester. *J. Aerosol Sci.* 27, S305-S306. [https://doi.org/10.1016/0021-8502\(96\)00225-X](https://doi.org/10.1016/0021-8502(96)00225-X)
- TSI, 1998. Estimation of Mass with the Model 3321 APS, tsi.com.
- Van Laarhoven, B., 2010. Breakage of Agglomerates: Attrition, Abrasion and Compression.
- Wang, H., John, W., 1987. Particle density correction for the aerodynamic particle sizer. *Aerosol Sci. Technol.*
- Yang, W.-C., 2003. Handbook of fluidization and fluid-particle systems, Chemical Engineering. [https://doi.org/10.1016/S1672-2515\(07\)60126-2](https://doi.org/10.1016/S1672-2515(07)60126-2)

8. List of figures

Error! Reference source not found. Particle size distribution of SiC samples F220 and F320. (a) by volume from laser diffraction analysis (b) by number from image analysis represented as relative distribution (in %).

Error! Reference source not found.

Error! Reference source not found. The error bars show the standard deviations calculated from three repeated trials. Vertical error bars are shown for both figures.

Error! Reference source not found. The error bars show the standard deviations calculated from three repeated trials.

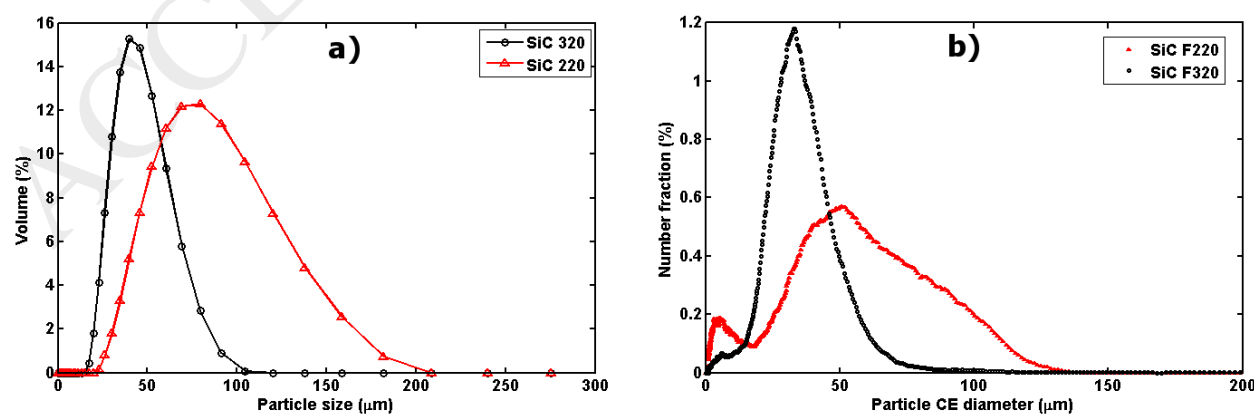
Error! Reference source not found. The error bars show the standard deviations calculated from three repeated trials.

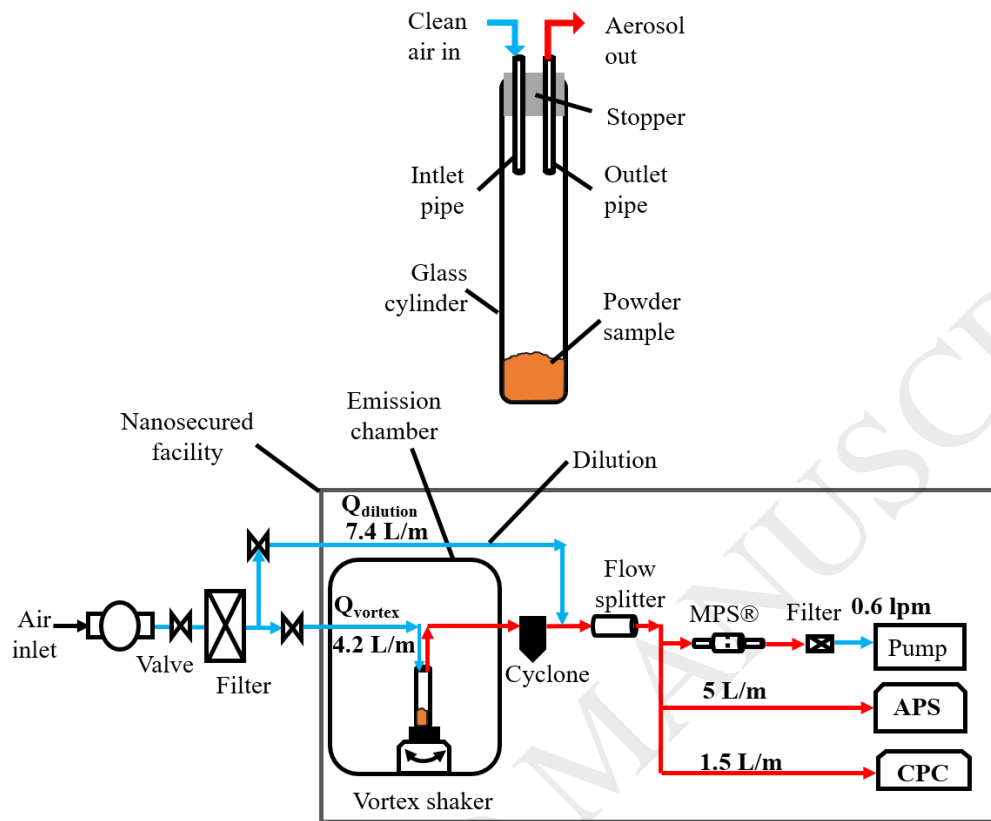
Error! Reference source not found. captured at 25th- 30th minute interval and from 350th minute - 360th minute interval.

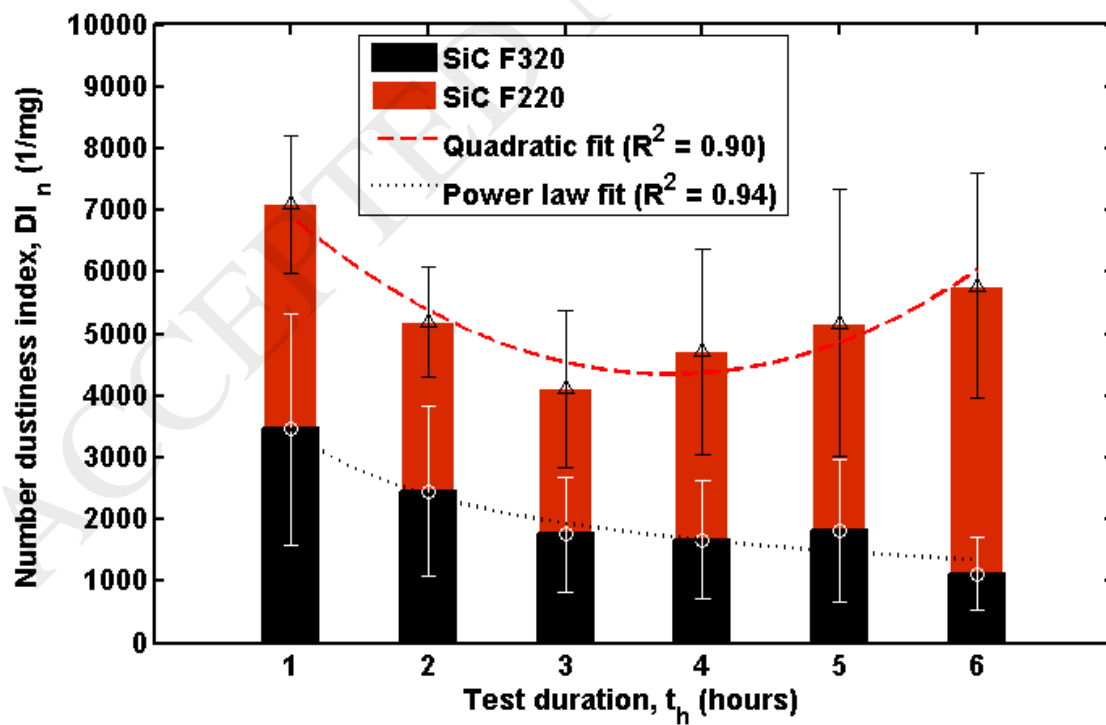
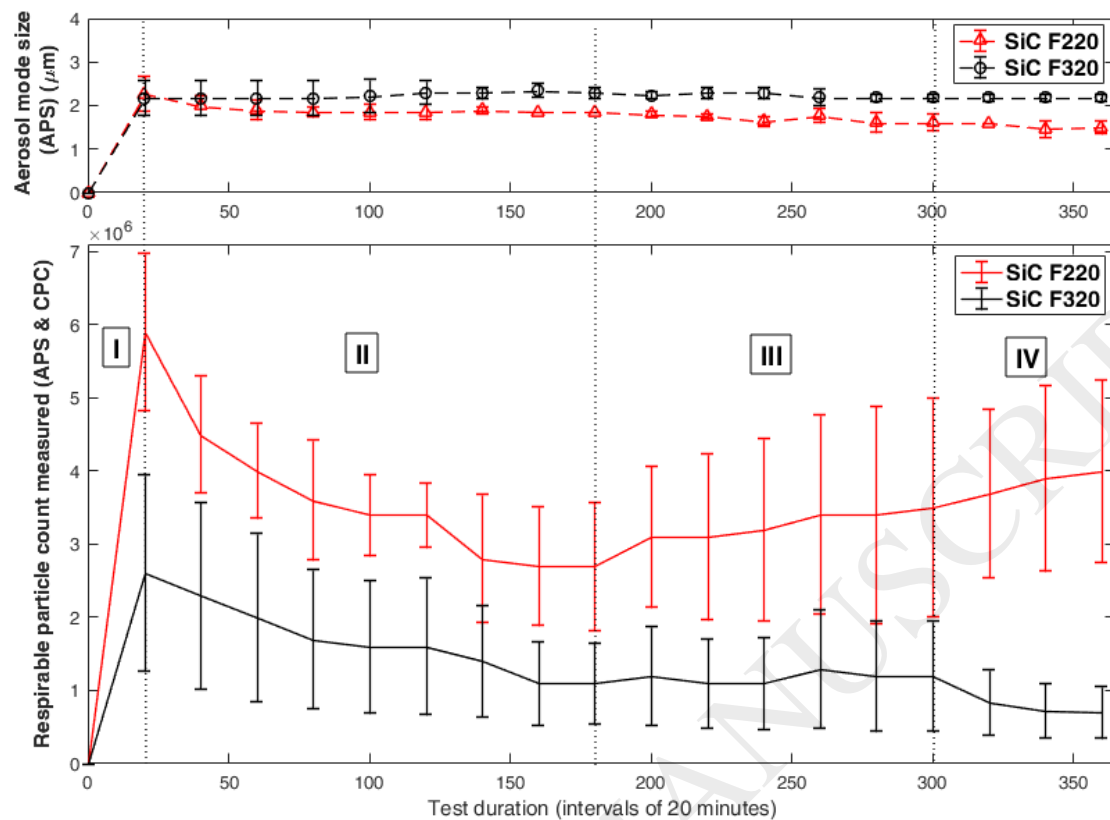
Error! Reference source not found. Changes in F220 (F220 and F220_tested) was more prominent than F320 (F320 and F320_tested).

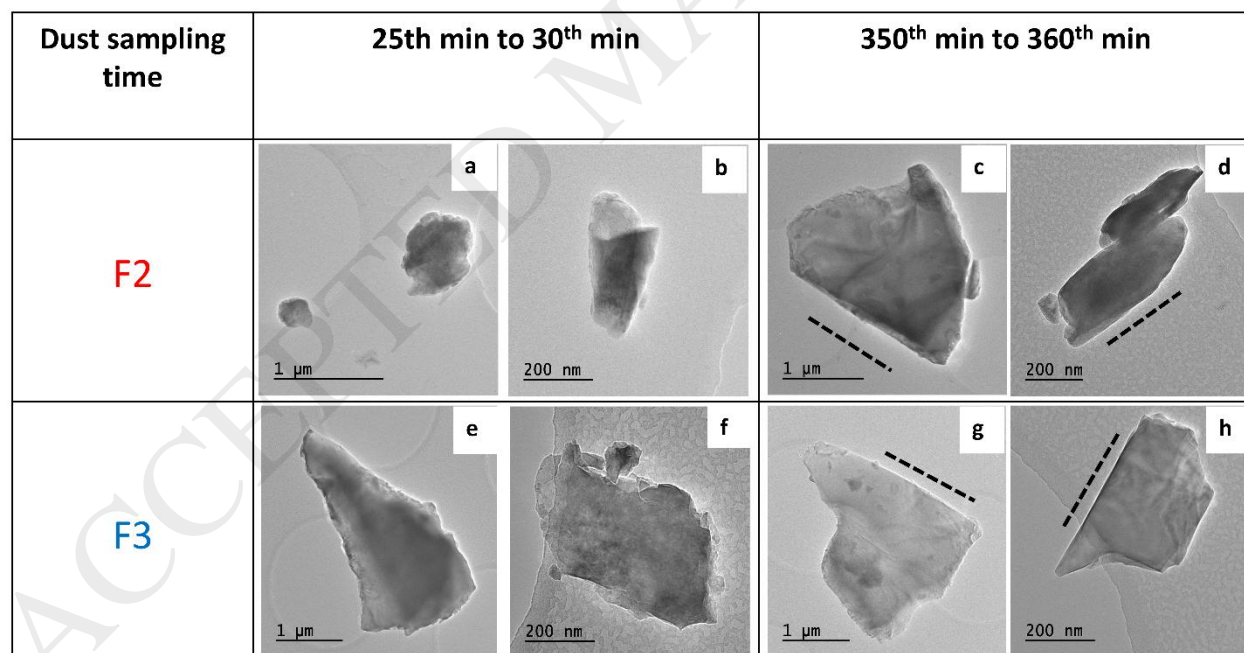
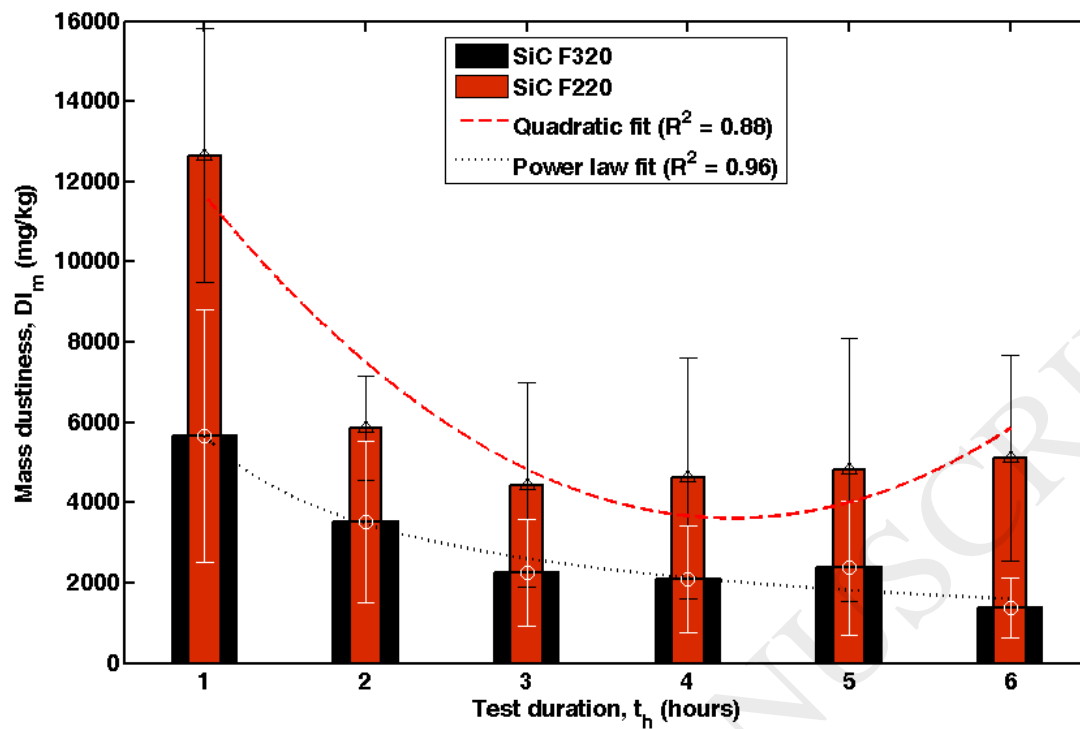
Error! Reference source not found.

Error! Reference source not found.

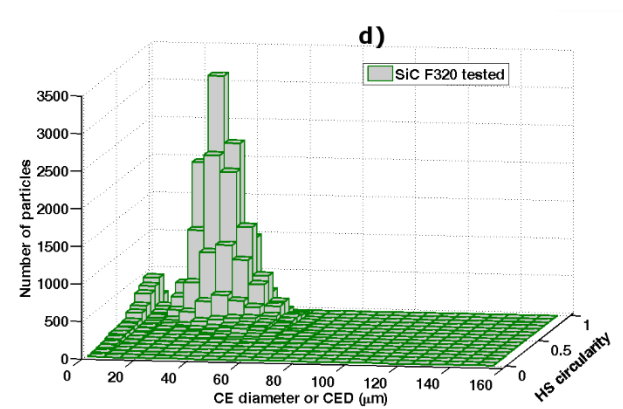
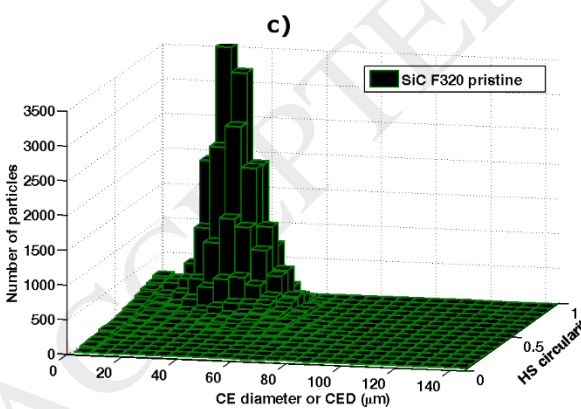
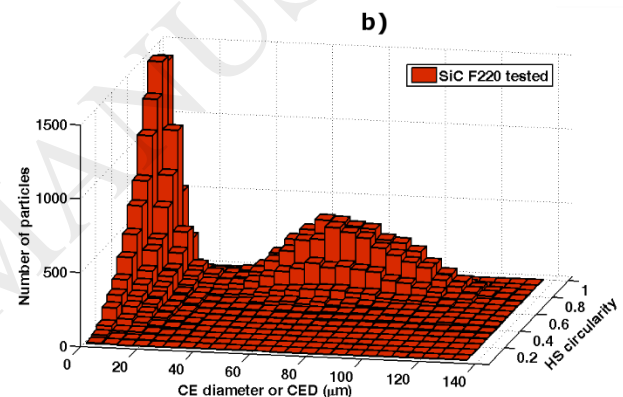
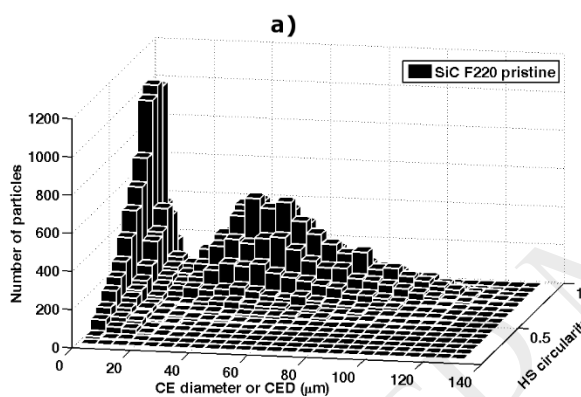
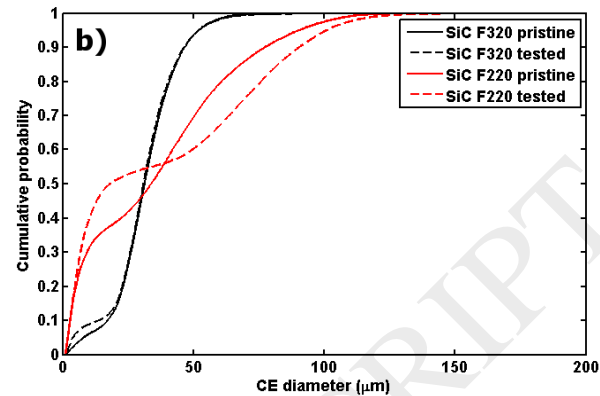
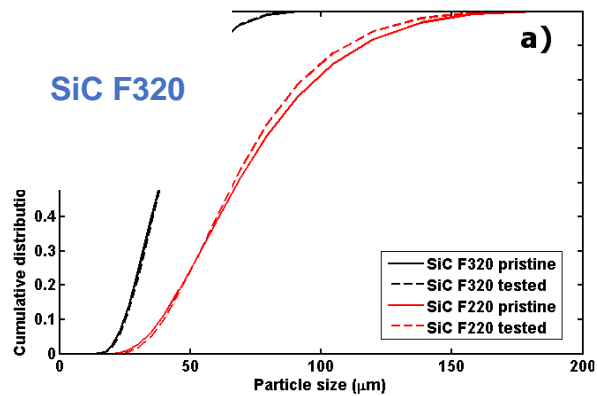


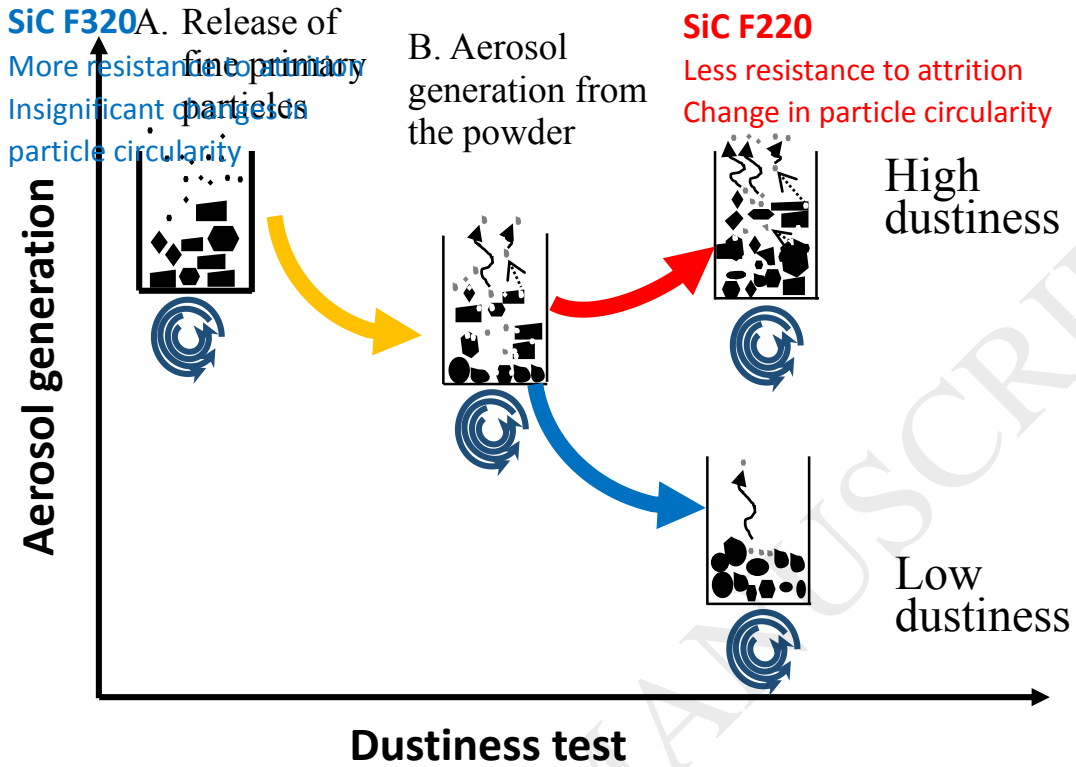






SiC F220





9. List of tables

Table 1

Powder properties of SiC F220 and F320 test samples.

	Units	F220	F320
Particle density ^a , ρ_p	kg/m ³	3,210	3,210
Size distribution by volume ^b	μm		
x_{10} (SD)		38.7 (0.02)	24.7 (0.04)
x_{50} (SD)		68.2 (0.08)	38.5 (0.06)
x_{90} (SD)		115 (0.15)	59.8 (0.11)
Span ^b $[(x_{90} - x_{10})/x_{50}]$	-	1.12	0.91
Surface weighted mean, D[3,2] ^b (SD)	μm	60 (0.18)	36 (0.02)
Specific surface area ^c	m ² /g	0.029	0.052
Moisture content ^d	%	< 0.1	< 0.1

^a Data provided by the manufacturer^b Three replicates were measured for each powder sample using Mastersizer 2000 laser particle size analyzer (Malvern Instruments, UK) for sizes 0.01 μm - 10,000 μm . The samples were stirred in de-mineralized water for 5 min before measuring.^c Nitrogen adsorption surface area analyzer (Micromeritics Gemini, Norcross, USA)^d Moisture content (by mass) measured using a halogen moisture analyzer (Mettler Toledo, USA)

Table 2 Volumetric PSD of the fresh (F220 and F320) and tested powder samples (F220_tested and F320_tested).

Table 2.

Volumetric PSD of the fresh (F220 and F320) and tested powder samples (F220_tested and F320_tested).

Test Samples	Distribution by volume			
	x_{10} (μm) (SD)	x_{50} (μm) (SD)	x_{90} (μm) (SD)	Span
F220	38.7 (0.02)	68.2 (0.08)	115 (0.15)	1.12
F220_tested	39.8 (0.01)	66.5 (0.02)	109 (0.6)	1.04
F320	24.7 (0.04)	38.5 (0.06)	59.8 (0.11)	0.91
F320_tested	25.3 (0.45)	38.9 (0.04)	59.5 (1.1)	0.88

Table 3 Particle size and shape factors for the fresh (F220 and F320) and tested (F220_tested and F320_tested) samples measured by particle number using image analysis.

Table 3.

Particle size (CED) and shape factors for the fresh (F220 and F320) and tested (F220_tested and F320_tested) samples measured based on particle number using image analysis.

Test Samples	x_{50} (in μm)	Mean HSC (SD) (max. 1)	Mean Convexity (SD) (max. 1)	Mean Aspect ratio (SD) (max. 1)
F220	35.68	0.70 (0.08)	0.97 (0.01)	0.62 (0.03)
F220_tested	18.11	0.74 (0.01)	0.97 (0.00)	0.66 (0.00)
F320	31.59	0.81 (0.01)	0.98 (0.00)	0.73 (0.01)
F320_tested	31.58	0.81 (0.01)	0.98 (0.00)	0.72 (0.01)